

Applied Mathematics and Nonlinear Sciences

<http://journals.up4sciences.org>

Photometric and Spectroscopic Studies of the Intermediate -Polar Cataclysmic System DQ Her

I. Zead¹, M. Saad¹, M. R. Sanad¹, M. M. Behary², K. Gadallah², A. Shokry^{1b}

1. National Research Institute of Astronomy and Geophysics (NRIAG)

Department of Astronomy, Stellar Lab., Helwan 11421, Cairo, EGYPT

2. Department of Astronomy, Faculty of Sciences,

El Azhar University, Cairo, EGYPT

Submission Info

Communicated by E.I. Abouelmagd

Received 5th March 2017

Accepted 23th May 2017

Available online 23th May 2017

Abstract

We report the results of spectral and photometric observations of DQ Her. Available spectra from International Ultraviolet Explorer (IUE), Hubble Space Telescope Faint Object Spectrograph (HST - FOS) and CCD photometry of one night were used. Some profiles revealing the variations of some spectral lines at different times are presented. There is variation with time for photometric observations and the brightness of DQ Her is changed from 14 mag. to 17.7 mag with clear display of burst. The ultraviolet luminosity for emitting region is in the range of $(1.9 \times 10^{31} \text{ erg s}^{-1})$. The mass accretion rate is in the range of $(3.5 \times 10^{-12} M_{\odot} \text{ yr}^{-1})$. The line flux modulations at different times can be explained in terms of the accretion curtain model for intermediate polars, Kim & Beuermann (1996).

Keywords: Photometric, spectroscopic studies, polar cataclysmic system, celestial dynamics.

AMS 2010 codes: 37N05, 70F15.

1 Introduction

Cataclysmic variables with magnetic white dwarf whose magnetic field is not strong enough to synchronize the white dwarf spin with the orbit of the system are known as intermediate polars (IPs).

In the intermediate polars, the white dwarf star has a small magnetic field less than 10 MG, so a complete accretion disk cannot be formed. Intermediate polars reveal periodic variations that reflect the orbital period of the binary system and the spin period of the primary star. The asynchronous rotation of white dwarfs in

^b Corresponding author.

Email address: z_ibrahim_zead@yahoo.com

IPs can be interpreted by the reaction between the magnetic field of the white dwarf and the disk matter near the magnetosphere. More details can be found in Warner [34], Patterson [24], Hellier [11], Warner [33], and Campbell [4].

DQ Her (Nova Herculis 1934) was first detected at its bright phase with a magnitude of ~ 3.3 mag (c.f. [5]). DQ Her is a prototype of an intermediate Polar stars, and also is a moderately slow galactic nova. DQ Her is a binary system contains a white dwarf with an intermediate magnetic field which can partially control the accreting stream from the red dwarf along the magnetic field lines to fall onto one or both magnetic poles of the white dwarf [25]. It is also characterized by Thermonuclear Runaway (TNR) on the surface of the white dwarf [31]. Walker [32] was discovered the eclipsing behavior of DQ Her and reported a consistent 71 sec. photometric oscillation. The spectral type of the dwarf is estimated to be M3 due to the detection of faint TiO bands between $\lambda\lambda$ 7150 Å to 7700 Å (Young & Schneider [38]). Since DQ Her is an eclipsing binary with an orbital period of 4^h39^m and has been extensively observed, its properties are well known, and estimated masses for its components are $0.6 M_{\odot}$ and $0.4 M_{\odot}$ for M_1 and M_2 , respectively (Horne et al. [12]).

The mass transfer in DQ Her was detected by Kraft [16]. Mumford [19] and Nather & Warner [20] suggested an increase in DQ Her orbital period. Later on (Patterson et al. [23]; Africano & Olson [1]; Zhang et al. [39]; Wood et al. [35]) indicated modulation of 14 yr period. However, an updated O-C analysis done by Wood et al. [35] found no evidence for a secular orbital period increase.

DQ Her is one of the most studied classical novae. Its maximum brightness recorded in 1934 with $m_V = 1.3$ while its post outburst magnitude was $m_V = 14.3$ (Duerbeck [7]) and it located at distance of 400 pc. The main characteristics of all DQ Her systems have been reviewed by Patterson [24]. According to the model discussed by Chanan et al. [6], a beam of X-ray and UV photons originating at the polar caps of the rotating WD moves around and illuminating the surface of the concave disk where the 71 sec. optical pulses originate. The 71 sec. stable pulsations are also observed in the $HeII$ λ 4686 line (Chanan et al. [6]; Martell et al. [17]), in the UV continuum and several UV emission lines (Silber et al. [29]), but not in the X-ray band (Silber et al. [28]; Mukai et al. [18]). DQ Her is a surprisingly faint X-ray source (Orio et al. [22]). The most recent ephemeris of the DQ Her eclipsing binary system suggested a period of 4.6469 h (Zhang et al. [39]; Ogloza et al. [21]).

The first radial velocity measurements of DQ Her suggested both high-mass solutions with $M_1 = 1.1 M_{\odot}$ and $M_2 = 0.55 M_{\odot}$ (Robinson [26]; Hutchings et al. [14]), and low-mass solutions with $M_1 = 0.47 M_{\odot}$ and $M_2 = 0.34 M_{\odot}$ (Smak [30]; Young & Schneider [37]). Finally, the direct spectroscopic measurements of the cool secondary star allowed Horne et al. [12] to the more reliable estimates $M_1 = 0.60 M_{\odot}$, $M_2 = 0.40 M_{\odot}$ and $i = 86.5^\circ$; such a mass of the WD is required for a system exhibiting slow nova outbursts (Starrfield [31]). Horne et al. [12] also give $K_1 = 140 \text{ km/s}$, $K_2 = 227 \text{ km/s}$, $i = 86.5^\circ$, and a total eclipse width $\Delta\phi = 0.22P$.

2 Observations and data reductions

2.1 HST and IUE SWP low resolution spectra of DQ Her

The IUE low-resolution short wavelength spectra have been obtained from the INES (IUE Newly Extracted Spectra) site ^a The INES system for low-resolution data is fully described by Rodríguez-Pascual et al. [27] and González-Riestra et al. [8]. The observational data are The IUE spectra were examined in the wavelength region 1150 Å - 1950 Å and the most suitable features are identified for analysis. The available IUE observations for DQ Her covering most of the orbital phases. Tables 1, list the ultraviolet observations for DQ Her with low resolution and large aperture.

Due to lack of IUE spectra for DQ Her, Hubble Space Telescope (HST-FOS) observations of DQ Her have been collected from the Hubble Space Telescope center (MAST) at site ^a. For an explanation of the FOS spectrographs see Kimble et al. (1998); Woodgate et al. [36]; Harms and Fitch [9]. The Hubbel Space Telescope

^a <http://ines.vilspa.esa.es>.

^a <http://archive.stsci.edu>.

data were analyzed using the standard IRAF software package for the reduction and analysis of spectrum. We processed HST/FOS spectra of the DQ Her system using the G160L, G190H and G130H gratings and 1.0 aperture. HST observations are listed in the Table 2. Figs. 1, 2, and 3 represent the phase modulations of line fluxes. For DQ Her, the following ephemeris of Schneider and Greenstein (1979) has been used.

$$HJD = 2434954.94423 + 0.193620873 \times E \quad (1)$$

Table 1 List of IUE observations for DQ Her.

| Data ID | Exp Time(s) | HJD 2440000+ | Phase |
|----------|-------------|--------------|-------|
| SWP06358 | 5400 | 4118.934 | 0.55 |
| SWP06848 | 9900 | 4159.704 | 0.12 |
| SWP07408 | 10800 | 4222.544 | 0.67 |
| SWP09147 | 25200 | 4222.544 | 0.67 |
| SWP09201 | 22200 | 4396.614 | 0.70 |
| SWP17593 | 4800 | 5186.821 | 0.91 |
| SWP17614 | 7200 | 5188.652 | 0.36 |
| SWP17615 | 2400 | 5188.752 | 0.88 |
| SWP25440 | 1440 | 6137.675 | 0.81 |
| SWP25441 | 2400 | 6137.711 | 0.99 |
| SWP25442 | 3600 | 6137.768 | 0.29 |
| SWP27812 | 18300 | 6490.105 | 0.02 |

Table 2 List of HST observations for DQ Her.

| Data ID | Exp Time(s) | Gratings | HJD 2440000+ | Phase |
|-----------|-------------|----------|--------------|-------|
| Y1DZ0603T | 2400 | G190H | 49275.3442 | 0.34 |
| Y1DZ0602T | 2169.361 | G160L | 49275.27584 | 0.28 |
| Y1DZ0601T | 2169.361 | G160L | 49275.21044 | 0.21 |
| Y1DZ0501T | 2169.361 | G160L | 49275.15263 | 0.15 |
| Y2LU0604T | 2400 | G190H | 49834.92946 | 0.93 |
| Y2LU0603T | 1737.476 | G160L | 49834.85829 | 0.86 |
| Y2LU0602T | 1737.476 | G160L | 49834.7912 | 0.79 |
| Y2LU0601T | 1737.476 | G160L | 49834.72603 | 0.73 |
| Y2XPA103T | 2418.216 | G130H | 50003.3599 | 0.36 |
| Y2XPA102T | 2418.216 | G130H | 50003.29308 | 0.29 |
| Y2XPA104T | 2243.053 | G130H | 50003.4261 | 0.43 |
| Y2XPA101T | 1717.566 | G130H | 50003.23115 | 0.23 |
| Y2XPB203T | 2418.216 | G130H | 50007.45564 | 0.46 |
| Y2XPB202T | 2418.216 | G130H | 50007.38878 | 0.39 |
| Y2XPB201T | 2340.365 | G130H | 50007.32284 | 0.32 |
| Y2XPB204T | 2262.516 | G130H | 50007.52198 | 0.52 |

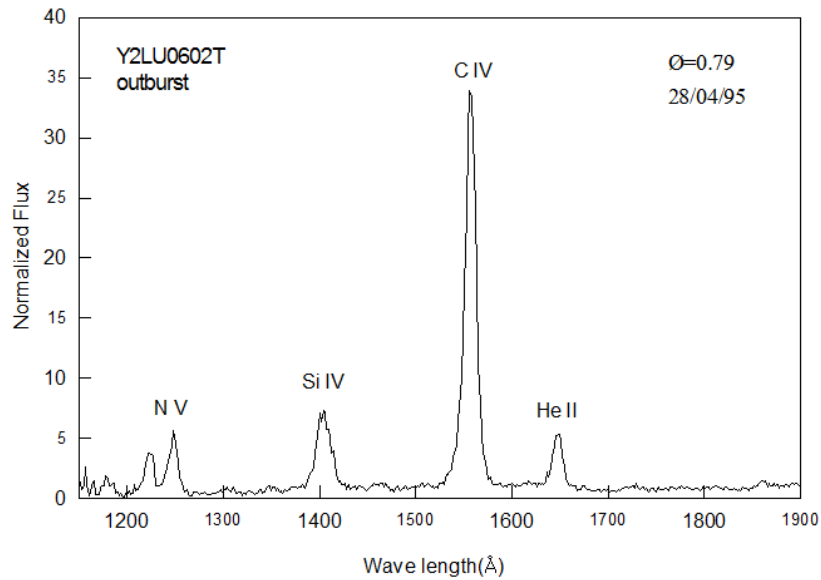


Fig. 1 HST spectrum of DQ Her with outburst flux at phase 0.79.

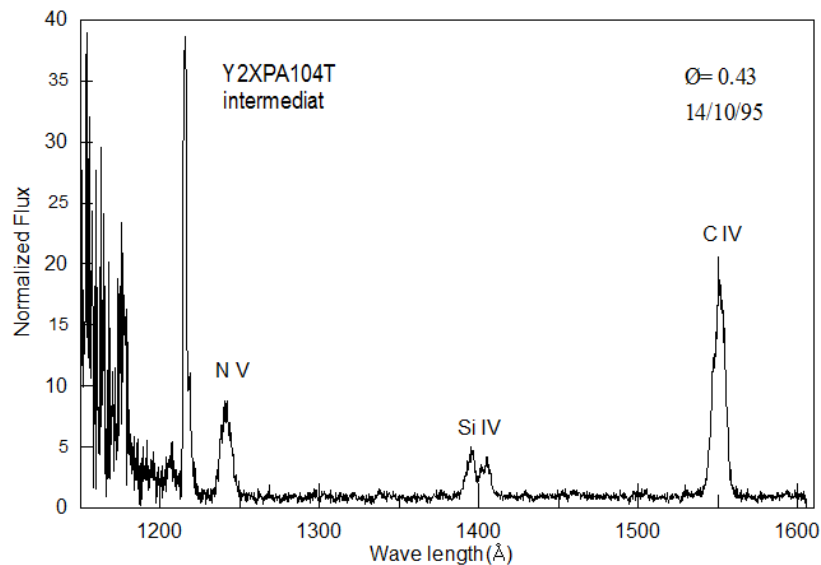


Fig. 2 HST spectrum of DQ Her with intermediate flux at phase 0.43.

2.2 CCD Photometric Observations of DQ Her

The CCD photometric observations of the target stars selected for the study are obtained using $2k \times 2k$ CCD camera attached to Newtonian focus of the 74 inch reflecting Telescope at Kottamia Astronomical Observatory (KAO), Cairo, Egypt. The CCD camera has a set of photometric filters (UBVRI). For DQ Her we obtained photometry in VRI filters.

Data reduction, where CCD observed frames (for the variable the comparison and the check stars) are corrected for bias and flat field is mainly performed using different tasks of IRAF software packages. Then we used the packages of C-Munipack program to do the photometry and extract the magnitude variability for each system by means of differential photometry.

Differential photometry is performed for measuring the small variations in brightness of the target variable star in comparison with other two non-variable stars known as comparison (C) and check stars (Ck). This

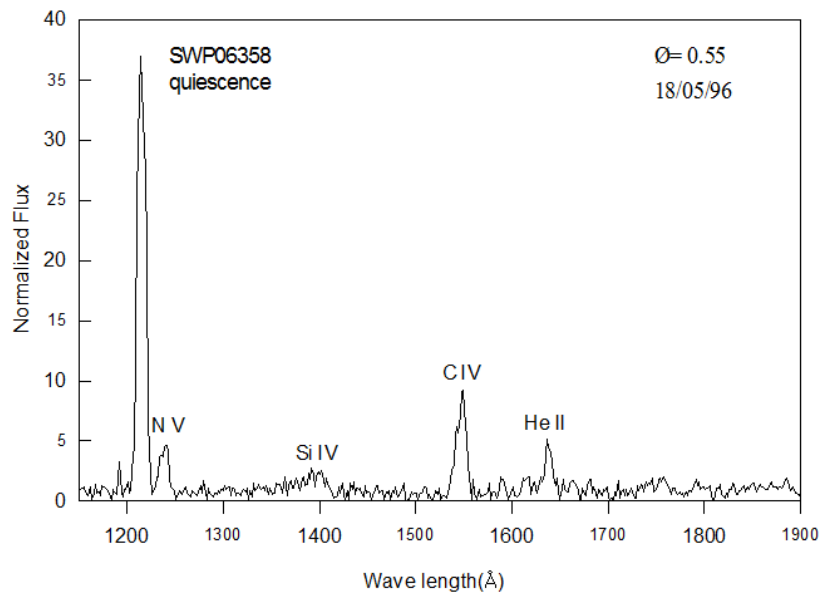


Fig. 3 IUE spectrum of DQ Her with quiescence flux at phase 0.55.

technique is widely used in variable stars, especially for short period variables and eclipsing binary systems. In differential photometry a comparison and a check stars together with the variable are exposed in the same CCD frame.

The photometric observations for DQ Her are obtained in V, R and I filters as shown in Tables (4), (5) and (6) respectively. Fig 4 displays the field chart of the system. The differential photometry was performed with respect to 000-BCB-330 and 000-BCB-348 as comparison and check stars respectively, Table 3 lists their coordinates. Fig 5 shows the phase diagrams for DQ Her in V, R and I filters folded with phase equation (1).

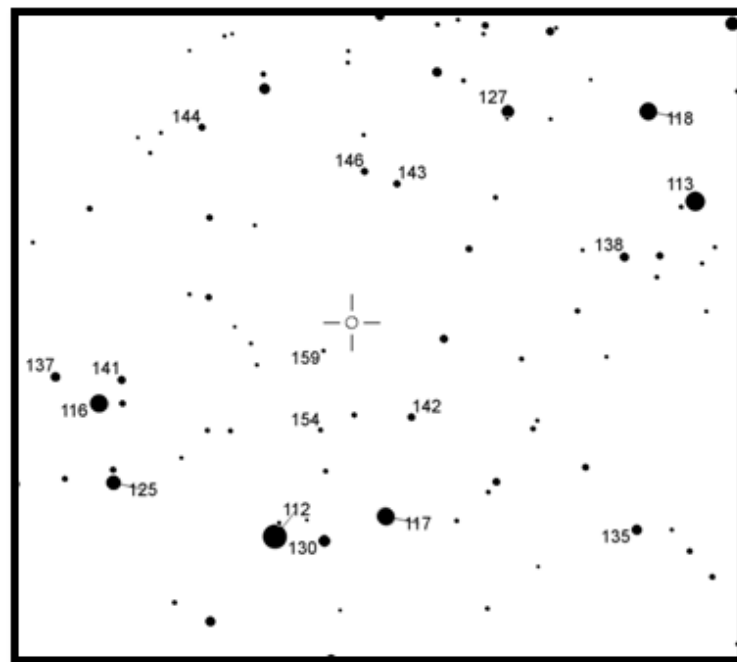


Fig. 4 The field chart of the DQ Her

Table 3 List of the comparison and the check of DQ Her.

| ID | RA | DEC | Label | M_v |
|-------------|-------------|------------|-------|--------|
| 000-BCB-330 | 18:07:23.97 | 45:49:47.6 | 142 | 14.231 |
| 000-BCB-348 | 18:07:33.58 | 45:49:33.5 | 154 | 15.375 |

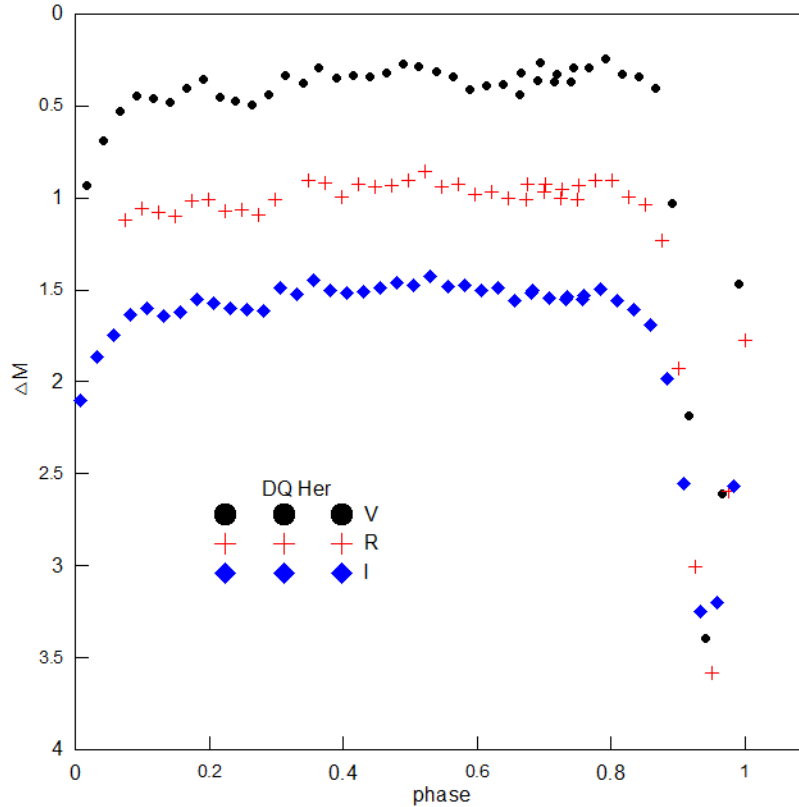


Fig. 5 the observed VRI phase diagrams of DQ HER folded with 4.6 day period.

3 Results and discussions

3.1 spectral behavior of the emission lines in DQ Her

The most obvious spectral lines features are seen in the spectra of the system: The high ionized C IV emission line at 1550 Å is a resonance doublet emission line, while He II 1640 Å is a recombination line, previously discussed by (Howell et al. [13]). These spectral lines are produced in the accretion curtain region as suggested by Bloemen et al. [2].

Figs. 8 and 9 reveal the spectral behavior of line fluxes with orbital phase for the C IV and He II, emission lines for DQ Her. The fluxes of spectral lines vary with orbital phases between high, intermediate and low values on short time scale of some hours and long time scale of some years. The behavior of C IV and H II line fluxes with orbital phase for DQ Her. The behavior are noted for DQ Her, since the line fluxes of C IV are the more intense one over the whole phases. Highly ionized C IV is vary by a factor of 4, while the fluxes of He II vary by a factor of 2. The maximum line fluxes of C IV and He II for DQ Her obviously seen around phase (0.1,0.85) while reached its least values around the orbital phase (0.3,1.0).

In this paper, we can explain the spectral variations in IUE and HST observations as shown in the figures (8& 9) by the following physical mechanisms. The emission lines of the intermediate polars (DQ Her) originated in

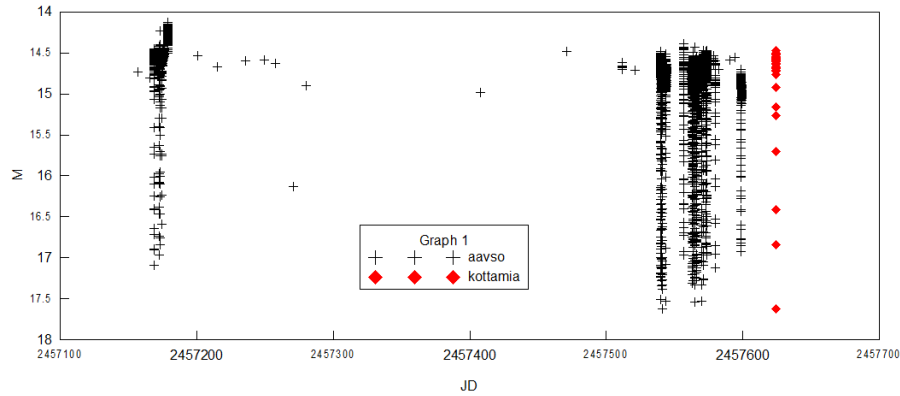


Fig. 6 Our CCD photometric observations in comparison with that collected from the AAVSO data base for DQ Her.

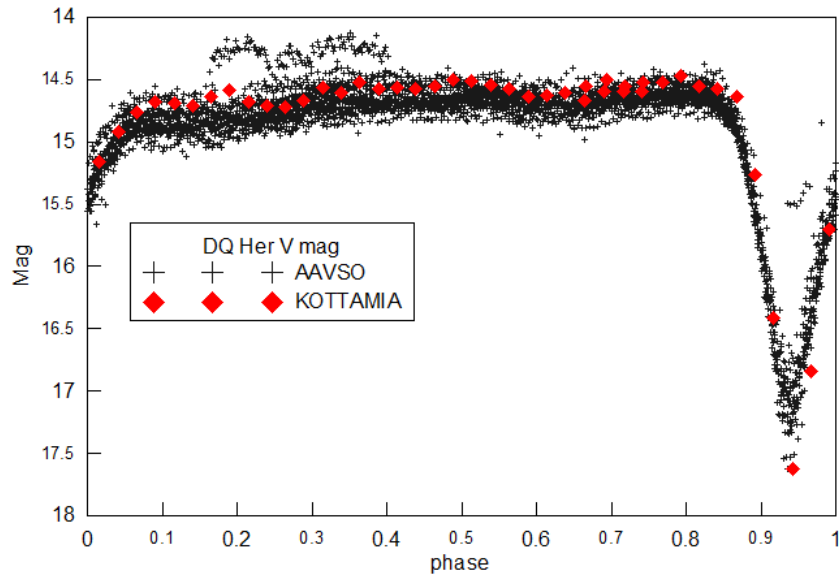


Fig. 7 DQ Her observed phase diagram in comparison with that collected from the AAVSO data base .

the accretion curtain region. The high energy photons in the emitting region produce the ultraviolet emission lines seen in this system. In this view, we can refer the luminosity of DQ Her to be correlated to the rate of its mass transfer and the origin of the ultraviolet spectral lines to the accretion curtain region. So as the rate of mass transfer increases, the gravitational potential energy increases, and this will lead to an increase in the temperature and consequently in the strength of ultraviolet spectral lines. The accretion curtain model for intermediate polars, Kim & Beuermann [15], Hellier et al. [10] and Buckley & Tuohy [3] support the results of current IUE & HST data as due an evidence of magnetically controlled accretion curtains near the white dwarf. The model described well the present spectral fluxes behavior of IUE and HST data for this system. In this model the emission lines seem to be originated in the region where the strength of the magnetic field prohibit the formation of the disk.

3.2 Photometric behavior of DQ Her

As shown from the fig our photometric observations almost covered the whole period of variations of DQ Her. The photometric variation of DQ Her revealed that the system is an eclipsing binary and the binary DQ Her shows variability with orbital period of ~ 4.6 hours caused by rotation of the white dwarf and the radiation emitted by the two magnetic poles. We see that light reprocessed through the accretion disk because we see the disk edge-on, and the white dwarf itself is obscured.

Table 4 list of CCD Photometry of DQ Her in V filter.

| JD 2457624+ | phase | v-c | JD 2457624+ | phase | v-c |
|-------------|-------|-------|-------------|-------|-------|
| 0.219 | 0.666 | 0.319 | 0.325 | 0.215 | 0.452 |
| 0.224 | 0.693 | 0.267 | 0.330 | 0.240 | 0.475 |
| 0.229 | 0.718 | 0.328 | 0.335 | 0.264 | 0.493 |
| 0.234 | 0.743 | 0.295 | 0.339 | 0.289 | 0.436 |
| 0.238 | 0.768 | 0.290 | 0.344 | 0.314 | 0.332 |
| 0.243 | 0.792 | 0.241 | 0.349 | 0.339 | 0.375 |
| 0.248 | 0.817 | 0.328 | 0.354 | 0.364 | 0.291 |
| 0.253 | 0.842 | 0.340 | 0.359 | 0.389 | 0.349 |
| 0.258 | 0.867 | 0.402 | 0.364 | 0.414 | 0.334 |
| 0.262 | 0.892 | 1.030 | 0.368 | 0.439 | 0.340 |
| 0.267 | 0.917 | 2.183 | 0.373 | 0.464 | 0.324 |
| 0.272 | 0.942 | 3.391 | 0.378 | 0.488 | 0.273 |
| 0.277 | 0.966 | 2.605 | 0.383 | 0.513 | 0.284 |
| 0.282 | 0.991 | 1.469 | 0.388 | 0.539 | 0.315 |
| 0.286 | 0.016 | 0.930 | 0.393 | 0.564 | 0.343 |
| 0.291 | 0.041 | 0.688 | 0.397 | 0.589 | 0.408 |
| 0.296 | 0.066 | 0.529 | 0.402 | 0.614 | 0.394 |
| 0.301 | 0.091 | 0.449 | 0.407 | 0.639 | 0.380 |
| 0.306 | 0.116 | 0.456 | 0.412 | 0.663 | 0.435 |
| 0.311 | 0.140 | 0.483 | 0.417 | 0.691 | 0.362 |
| 0.315 | 0.165 | 0.404 | 0.422 | 0.716 | 0.369 |
| 0.320 | 0.190 | 0.358 | 0.427 | 0.741 | 0.369 |

Fig. 6 represents all photometric observations collected through ~ 17 years at data base of the American Association of Variable Stars Observers (AAVSO). Different characteristic features of DQ Her variations, i.e., burst, super-burst, quiescent and narrow-burst can be detected well through Fig. 7 which shows the phase diagram of all observations for DQ Her. In both figures, the KAO photometry is in red.

3.3 Ultraviolet luminosity and accretion rate for DQ Her

For DQ Her, we used the integrated fluxes of emission lines C IV 1550 Å and He II 1640 Å, and equation (2), we obtained the variable ultraviolet luminosities for this spectral lines, it tabulated in Tables 7 and 8 using a mean distance value 400 pc, derived by Horne et al. [12].

$$L_{UV} = 2\pi F d^2 \quad (2)$$

For a white dwarf with $M_{wd} = 0.6M_{\odot}$ Horne et al. [12]. The radius of white dwarf $R_{WD} = 8.6 \times 10^8$ cm is calculated by using the equation (3), while the mass accretion rates are calculated by using the equation (4).

$$R_{WD} = 0.78 \times 10^9 \left[\left(\frac{1.44M_{\odot}}{M_{WD}} \right)^{2/3} - \left(\frac{M_{WD}}{1.44M_{\odot}} \right)^{2/3} \right]^{1/2} \quad (3)$$

$$\dot{M} = \frac{L_{acc} R_a}{GM_a} \quad (4)$$

Where M_a, R_a are the mass and radius of the accreting star, L_{acc} is the accretion luminosity, and G is the gravitational constant.

Table 5 list of CCD Photometry of DQ Her in R filter.

| JD 2457624+ | phase | v-c | JD 2457624+ | phase | v-c |
|-------------|-------|-------|-------------|-------|-------|
| 0.220 | 0.674 | 0.429 | 0.331 | 0.248 | 0.564 |
| 0.226 | 0.702 | 0.424 | 0.336 | 0.272 | 0.590 |
| 0.230 | 0.726 | 0.456 | 0.341 | 0.297 | 0.509 |
| 0.235 | 0.751 | 0.435 | 0.351 | 0.347 | 0.405 |
| 0.240 | 0.776 | 0.403 | 0.355 | 0.372 | 0.417 |
| 0.245 | 0.801 | 0.402 | 0.360 | 0.398 | 0.497 |
| 0.250 | 0.825 | 0.493 | 0.365 | 0.422 | 0.423 |
| 0.254 | 0.850 | 0.538 | 0.370 | 0.447 | 0.438 |
| 0.259 | 0.875 | 0.731 | 0.375 | 0.472 | 0.433 |
| 0.264 | 0.900 | 1.430 | 0.380 | 0.497 | 0.407 |
| 0.269 | 0.925 | 2.507 | 0.384 | 0.521 | 0.359 |
| 0.274 | 0.950 | 3.080 | 0.389 | 0.547 | 0.438 |
| 0.278 | 0.975 | 2.096 | 0.394 | 0.572 | 0.425 |
| 0.283 | 0.999 | 1.276 | 0.399 | 0.597 | 0.482 |
| 0.298 | 0.074 | 0.620 | 0.404 | 0.622 | 0.468 |
| 0.303 | 0.099 | 0.558 | 0.409 | 0.647 | 0.501 |
| 0.307 | 0.124 | 0.578 | 0.414 | 0.672 | 0.511 |
| 0.312 | 0.149 | 0.597 | 0.419 | 0.699 | 0.470 |
| 0.317 | 0.174 | 0.514 | 0.424 | 0.724 | 0.501 |
| 0.322 | 0.198 | 0.507 | 0.428 | 0.749 | 0.509 |
| 0.327 | 0.223 | 0.574 | | | |

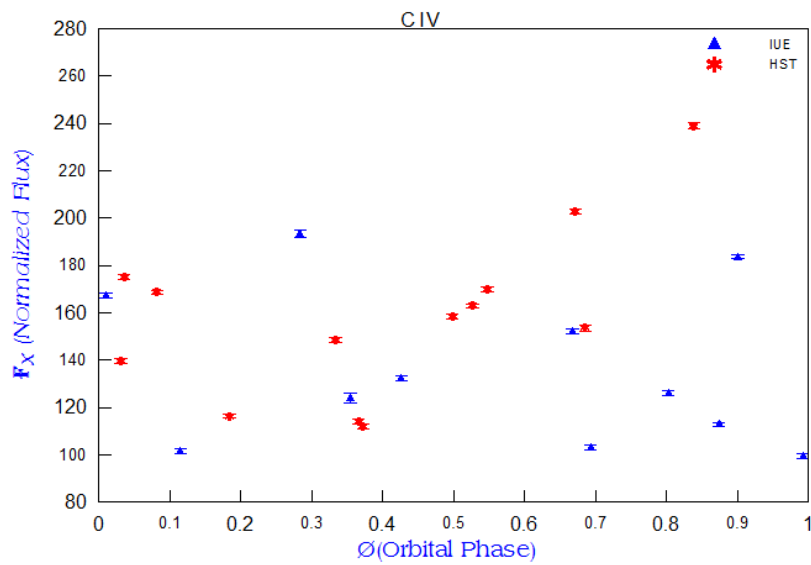


Fig. 8 Variation of the C IV line flux with phase of DQ Her The 1σ error bars are shown on each data point.

Table 6 list of CCD Photometry of DQ Her in I filter.

| JD 2457624+ | phase | v-c | JD 2457624+ | phase | v-c |
|-------------|-------|-------|-------------|-------|-------|
| 0.222 | 0.683 | 0.504 | 0.333 | 0.256 | 0.609 |
| 0.232 | 0.735 | 0.537 | 0.338 | 0.281 | 0.614 |
| 0.237 | 0.759 | 0.528 | 0.343 | 0.306 | 0.487 |
| 0.242 | 0.784 | 0.496 | 0.347 | 0.330 | 0.523 |
| 0.246 | 0.809 | 0.556 | 0.352 | 0.356 | 0.447 |
| 0.251 | 0.833 | 0.610 | 0.357 | 0.380 | 0.503 |
| 0.256 | 0.858 | 0.689 | 0.362 | 0.406 | 0.517 |
| 0.261 | 0.883 | 0.984 | 0.367 | 0.430 | 0.511 |
| 0.266 | 0.908 | 1.556 | 0.372 | 0.455 | 0.491 |
| 0.270 | 0.933 | 2.246 | 0.376 | 0.480 | 0.461 |
| 0.275 | 0.958 | 2.203 | 0.381 | 0.505 | 0.472 |
| 0.280 | 0.983 | 1.570 | 0.386 | 0.529 | 0.429 |
| 0.285 | 0.008 | 1.104 | 0.391 | 0.556 | 0.485 |
| 0.290 | 0.033 | 0.866 | 0.396 | 0.580 | 0.476 |
| 0.295 | 0.057 | 0.748 | 0.401 | 0.605 | 0.505 |
| 0.299 | 0.083 | 0.636 | 0.405 | 0.630 | 0.490 |
| 0.304 | 0.107 | 0.599 | 0.410 | 0.655 | 0.556 |
| 0.309 | 0.132 | 0.643 | 0.415 | 0.680 | 0.520 |
| 0.314 | 0.157 | 0.619 | 0.420 | 0.708 | 0.545 |
| 0.319 | 0.182 | 0.551 | 0.425 | 0.732 | 0.551 |
| 0.323 | 0.206 | 0.575 | 0.430 | 0.757 | 0.548 |
| 0.328 | 0.231 | 0.603 | | | |

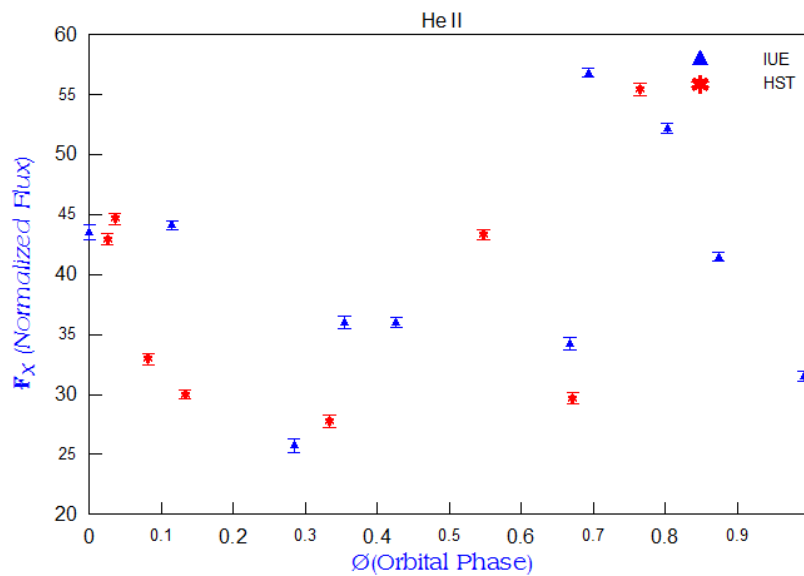


Fig. 9 Variation of the He II line flux with phase of DQ Her The 1 σ error bars are shown on each data point.

Table 7 Ultraviolet luminosities and accretion rate for the spectral line C IV (1550Å).

| State | Flux | L_{acc} | | \dot{M} |
|--------------|--|---------------------------------------|-------------------------------------|--|
| High | 4.09×10^{-12} (erg $cm^{-2} s^{-1}$) | 3.95×10^{31} (erg s^{-1}) | 4.5×10^{14} (g s^{-1}) | $7.17 \times 10^{-12} M_{\odot} yr^{-1}$ |
| Intermediate | 1.3×10^{-12} (erg $cm^{-2} s^{-1}$) | 1.3×10^{31} (erg s^{-1}) | 1.44×10^{14} (g s^{-1}) | $2.29 \times 10^{-12} M_{\odot} yr^{-1}$ |
| Low | 5.3×10^{-13} (erg $cm^{-2} s^{-1}$) | 5.13×10^{30} (erg s^{-1}) | 5.85×10^{13} (g s^{-1}) | $9.32 \times 10^{-13} M_{\odot} yr^{-1}$ |

Table 8 Ultraviolet luminosities and accretion rate for the spectral line He II (1640Å).

| State | Flux | L_{acc} | | \dot{M} |
|--------------|--|---------------------------------------|-------------------------------------|--|
| High | 4.32×10^{-13} (erg $cm^{-2} s^{-1}$) | 4.18×10^{30} (erg s^{-1}) | 4.8×10^{13} (g s^{-1}) | $7.65 \times 10^{-13} M_{\odot} yr^{-1}$ |
| Intermediate | 2.8×10^{-13} (erg $cm^{-2} s^{-1}$) | 2.7×10^{30} (erg s^{-1}) | 3.08×10^{13} (g s^{-1}) | $4.91 \times 10^{-13} M_{\odot} yr^{-1}$ |
| Low | 1.98×10^{-13} (erg $cm^{-2} s^{-1}$) | 1.9×10^{30} (erg s^{-1}) | 2.18×10^{13} (g s^{-1}) | $3.47 \times 10^{-13} M_{\odot} yr^{-1}$ |

4 Conclusions

We report the results of the photometric and spectroscopic behavior of DQ Her. The photometric analysis of DQ Her is performed using the CCD photometry of KAO and that collected over long time through AAVSO data base. The main results for the system can be summarized as:

- Photometry of DQ Her revealed that the system is an eclipsing binary with high inclination deg.
- KAO photometry and that collected from AAVSO are obviously comparable.
- The light variation reveal very deep primary minimum (where, main sequence component lie in front of the white dwarf) 17.7 mag., no secondary minima has been detected due to the dominant flux of the massive component.
- The intermediate Polar system DQ Herculis, in which the white dwarf is gravitationally stripped the matter from the main-sequence companion star and forms an accretion disk around the white dwarf and the inner disk region is truncated by the magnetic field of the white dwarf.
- In the region where the disk is truncated, the gas in the disk begins to transfer along the white dwarf's magnetic field lines, forming curved sheets of luminous material called accretion curtains. Disk material passes through the curtains and then accretes onto the white dwarf near one of its magnetic poles.
- The study revealed the presence of periodic and/or semi-periodic changes in the brightness of this system. One periodicity is related to the orbital period of the binary star system. A second periodic signal originates from the rotation of the white dwarf spinning on its axis and it is shorter than the orbital period. The observational characteristic that clearly defines this system is the existence of more than one overlap period which appear in general as irregular variables. The physical cause of optical spin period oscillations may be attributed to the changing viewing aspect of the accretion curtain as it converges near the white dwarf.
- Identification of emission lines in the spectral region 1150 Å - 1950 Å with detailed description of continuum and profiles.
- There are variations in the ultraviolet luminosities and the mass accretion rates.
- There are modulations in line fluxes for all studied emission lines (C IV and He II), we attributed these variations to the variations of the rate of mass transfer from the secondary star to the white dwarf leading to variation in temperature and consequently to the variations in the intensities of emission lines.
- The variations in both ultraviolet luminosities and the mass accretion rates in this system can be interpreted in terms of the accretion curtain model.

Acknowledgements. This research has made use of NASA's Astrophysics Data System. The research granted by Science and Technology Development Fund (STDF) N5217. We are very grateful the team of Kottamia Astronomical Observatory, Dr. F. I. El-Nagahy, M. Ismail, Doaa El-Sayed I. Helmy. We would like to give thanks to Dr. M. Hassan, Dr. N. M. Ahmed, A. Shokry, D. Fouda , G. M. N. Hamed, M. H. El-Depsy and M. S. Darwish for their fruitful discussions and help.

References

- [1] J. L. Africano and E. C. Olson, (1981), *Eclipse timings of DQ Herculis*, Publications of the Astronomical Society of the Pacific, 93, No 551, 130-133. doi [10.1086/130790](https://doi.org/10.1086/130790)

- [2] S. Bloemen et al., (2010), *Spin-resolved spectroscopy of the intermediate polar DQ Her*, Monthly Notices of the Royal Astronomical Society, 407, No 3, 1903-1912. doi [10.1111/j.1365-2966.2010.17035.x](https://doi.org/10.1111/j.1365-2966.2010.17035.x)
- [3] D. A. H. Buckley and I. R. Tuohy, (1989), *A spectroscopic, photometric, and X-ray study of the DQ Herculis system IH0542-407*, The Astrophysical Journal, 344, 376-398. doi [10.1086/167806](https://doi.org/10.1086/167806)
- [4] C. G. Campbell, (1997), *Magnetohydrodynamics in Binary Stars*, Astrophysics & Space Science Library, Vol. 216, Springer Netherlands. doi [10.1007/978-1-4020-0377-6](https://doi.org/10.1007/978-1-4020-0377-6)
- [5] L. Campbell, (1935), *Light Curve of Nova Herculis, 180445*, Harvard College Observatory Bulletin, 898, 20-25.
- [6] G. A. Chanan, J.E. Nelson and B. Margon, (1978), *Time-resolved spectrophotometry of DQ Herculis: A wavelength-dependent phase shift in 71 second pulsations of He II λ 4686*, The Astrophysical Journal, 226, 963-975. doi [10.1086/156677](https://doi.org/10.1086/156677)
- [7] H. W. Duerbeck, (1987), Errata: "A reference catalogue and atlas of galactic novae", Space Science Reviews, Vol. 45, No. 3-4, p. 405.
- [8] R. González-Riestra R., A. Cassatella and W. Wamsteker, (2001), *IV. The IUE absolute flux scale*, in: The INES system, Astronomy & Astrophysics, 373, 730-745. doi [10.1051/0004-6361:20010646](https://doi.org/10.1051/0004-6361:20010646)
- [9] R. J. Harms and J. E. Fitch, (1991), *Faint object spectrograph early performance*, in: Proc. SPIE 1494, Space Astronomical Telescopes and Instruments, 49 (September 1, 1991). doi [10.1117/12.46713](https://doi.org/10.1117/12.46713)
- [10] C. Hellier, M. Cropper and K. O. Mason, (1991), *Optical and X-ray observations of AO Piscium and the origin of the spin pulse in intermediate polars*, Monthly Notices of the Royal Astronomical Society, 248, No 2, 233-255. doi [10.1093/mnras/248.2.233](https://doi.org/10.1093/mnras/248.2.233)
- [11] C. Hellier, (2001), *Cataclysmic Variable Stars. How and why they vary*, Springer-Verlag, London.
- [12] K. Horne, W. F. Welsh and R. A. Wade, (1993), *On the mass of nova DQ Herculis (1934)*, The Astrophysical Journal, 410, No 1, 357-364. doi [10.1086/172752](https://doi.org/10.1086/172752)
- [13] S. B. Howell, et al., (1999), *The Relationship between Ultraviolet Line Emission and Magnetic Field Strength in Magnetic Cataclysmic Variables*, The Astronomical Journal, 117, No 2, 1014-1022. doi [10.1086/300740](https://doi.org/10.1086/300740)
- [14] J B. Hutchings, A. P. Cowley and D. Crampton, (1979), *The interactive binary in Nova DQ Herculis*, Astrophysical Journal, Part 1, Vol. 232, 500-509. doi [10.1086/157309](https://doi.org/10.1086/157309)
- [15] Y. Kim and K. Beuermann, (1996), *Spin-modulated radiation of intermediate polars. II. Optical light curves and H β line profiles.*, Astronomy and Astrophysics, 307, 824-828.
- [16] R. P. Kraft, (1959), *The Binary System Nova DQ Herculis. II. an Interpretation of the Spectrum during the Eclipse Cycle*, Astrophysical Journal, 130, 110-122. doi [10.1086/146701](https://doi.org/10.1086/146701)
- [17] P. J. Martell et al., (1995), *Taking the Pulse of DQ Herculis*, Astrophysical Journal, 448, 380-394. doi [10.1086/175969](https://doi.org/10.1086/175969)
- [18] K. Mukai, M. Still and F. A. Ringwald, (2003), *The Origin of Soft X-Rays in DQ Herculis*, The Astrophysical Journal, 594, 428-434. doi [10.1086/376752](https://doi.org/10.1086/376752)
- [19] G. S. Mumford, (1969), *Further Photometry of EX Hydrae*, Astrophysical Journal, 156, 125-134. doi [10.1086/149953](https://doi.org/10.1086/149953)
- [20] R. E. Nather and B. Warner, (1969), *DQ Herculis: Synchronous Photometry*, Science, 166, No 3907, 876-877. doi [10.1126/science.166.3907.876](https://doi.org/10.1126/science.166.3907.876)
- [21] W. Ogloza, M. Drozd and S. Zola, (2000), *Photoelectric Minima of Eclipsing Binaries*, Information Bulletin on Variable Stars, 4877, No 1, 4877, 1-2.
- [22] M. Orío et al., (2001), *A BeppoSAX observation of Nova Velorum 1999: A very bright classical Nova*, AIP Conference Proceedings, 599, 466-469. doi [10.1063/1.1434663](https://doi.org/10.1063/1.1434663)
- [23] J. Patterson, E. L. Robinson and R. E. Nather, (1978), *Title: Rapid oscillations in cataclysmic variables. I - The 71 second oscillation of DQ Herculis*, Astrophysical Journal, Part 1, 224, 570-583. doi [10.1086/156405](https://doi.org/10.1086/156405)
- [24] J. Patterson, (1994), *Energy Balance and Emission Lines in DQ Herculis Stars Cycle 4 - Medium*, HST Proposal ID #5500. Cycle 4.
- [25] J. Patterson, (1994), *The DQ Herculis Stars*, Publications of the Astronomical Society of the Pacific, 106, No 697, 209-238.
- [26] E. L. Robinson, (1976), *The masses of cataclysmic variables*, Astrophysical Journal, 203, 485-489. doi [10.1086/154103](https://doi.org/10.1086/154103)
- [27] P. M. Rodríguez-Pascual et al., (1999), *The IUE INES System: Improved data extraction procedures for IUE*, Astronomy & Astrophysics Supplement Series, 139, 183-197. doi [10.1051/aas:1999388](https://doi.org/10.1051/aas:1999388)
- [28] A. D. Silber et al., (1996), *Time Resolved Ultraviolet Spectroscopy of DQ Herculis: Eclipses and Pulsations*, Astronomical Journal, 112, 1174-1179. doi [10.1086/118087](https://doi.org/10.1086/118087)
- [29] A. D. Silber et al., (1996), *The Ultraviolet Spectrum of DQ Herculis: Detection of Line and Continuum Pulsation*, Astrophysical Journal, 462, 428-438. doi [10.1086/177162](https://doi.org/10.1086/177162)
- [30] J. Smak, (1980), *Eruptive binaries. X - DQ Herculis*, Acta Astronomica, 30, No 3, 267-283.
- [31] S. Starrfield, (1989), *Thermonuclear processes and the classical nova outburst*, Classical Novae, 39-60.
- [32] M. F. Walker, (1956), *A Photometric Investigation of the Short-Period Eclipsing Binary, Nova DQ Herculis (1934)*, Astrophysical Journal, 123, 68-89. doi [10.1086/146132](https://doi.org/10.1086/146132)
- [33] B. Warner, (2005), *Intermediate Polars in Low States*, in: White Dwarfs: Cosmological and Galactic Probes, Volume 332 of the series Astrophysics and Space Science Library pp. 211-215. doi [10.1007/1-4020-3725-2_20](https://doi.org/10.1007/1-4020-3725-2_20)

- [34] B. Warner, (1995), *Transitions to and from Stable Discs in Cataclysmic Variable Stars*, *Astrophysics and Space Science*, 230, No 1-2, 83-94. doi [10.1007/BF00658170](https://doi.org/10.1007/BF00658170)
- [35] M. A. Wood et al., (2005), *DQ Herculis in Profile: Whole Earth Telescope Observations and Smoothed Particle Hydrodynamics Simulations of an Edge-on Cataclysmic Variable System*, *The Astrophysical Journal*, 634, No 1, 570-584. doi [10.1086/496957](https://doi.org/10.1086/496957)
- [36] B. E. Woodgate et al., (1998), *The Space Telescope Imaging Spectrograph Design*, *Publications of the Astronomical Society of the Pacific*, 110, No 752, 1183-1204. doi [10.1086/316243](https://doi.org/10.1086/316243)
- [37] P. Young and D. P. Schneider, (1980), *Emission line eclipse phenomena in nova DQ Herculis /1934/*, *Astrophysical Journal*, Part 1, 238, 955-963. doi [10.1086/158060](https://doi.org/10.1086/158060)
- [38] P. Young and D. P. Schneider, (1981), *A quest for the red companion in six cataclysmic binaries*, *Astrophysical Journal*, Part 1, 247, 960-968. doi [10.1086/159105](https://doi.org/10.1086/159105)
- [39] E. Zhang et al., (1995), *The 71 Second Oscillation in the Light Curve of the Old Nova DQ Herculis*, *Astrophysical Journal*, 454, 447-462. doi [10.1086/176496](https://doi.org/10.1086/176496)

©UP4 Sciences. All right reserved.